Excitation Energy-Transfer and the Relative Orientation of Retinal and Carotenoid in Xanthorhodopsin

Sergei P. Balashov, Eleonora S. Imasheva, Jennifer M. Wang, and Janos K. Lanyi
Department of Physiology and Biophysics, University of California, Irvine, California

ABSTRACT   The cell membrane of *Salinibacter ruber* contains xanthorhodopsin, a light-driven transmembrane proton pump with two chromophores: a retinal and the carotenoid, salinixanthin. Action spectra for transport had indicated that light absorbed by either is utilized for function. If the carotenoid is an antenna in this protein, its excited state energy has to be transferred to the retinal and should be detected in the retinal fluorescence. From fluorescence studies, we show that energy transfer occurs from the excited singlet S_2 state of salinixanthin to the S_1 state of the retinal. Comparison of the absorption spectrum with the excitation spectrum for retinal emission yields $45 \pm 5\%$ efficiency for the energy transfer. Such high efficiency would require close proximity and favorable geometry for the two polyene chains, but from the heptahelical crystallographic structure of the homologous retinal protein, bacteriorhodopsin, it is not clear where the carotenoid can be located near the retinal. The fluorescence excitation anisotropy spectrum reveals that the angle between their transition dipole moments is $56 \pm 3°$. The protein accommodates the carotenoid as a second chromophore in a distinct binding site to harvest light with both extended wavelength and polarization ranges. The results establish xanthorhodopsin as the simplest biological excited-state donor-acceptor system for collecting light.

INTRODUCTION

The majority of energy resources on Earth originate from light captured by biological organisms and transformed in the processes of photosynthesis. Evolution has augmented energy-transducing photosystems with additional pigments that function as antennae. Excitation energy transfer is an essential part of light harvesting. Chlorophyll-to-chlorophyll and carotenoid-to-chlorophyll energy transfer, widely utilized in the light-harvesting complexes of photosynthetic organisms to increase spatial and spectral range of light absorption (1–3), involves tens and hundreds of interacting chromophores and several excited states of both donor and acceptor including the extremely short-lived S_2 state of the carotenoids (4–7), responsible for their intense absorption bands (8,9). A much simpler system, the small retinal protein xanthorhodopsin containing just one donor and one acceptor, was found recently in cell membranes of the extremely halophilic eubacterium *Salinibacter ruber* (10).

Bacteriorhodopsin, an earlier evolved retinal-based light energy transducer of the archaea, lacks an antenna (11,12). However, energy transfer has been proposed to occur in other retinal proteins. Examples include retinol-enhanced sensitivity of fly rhodopsin to ultraviolet light (13,14) and possibly a porphyrin-enhanced photoresponse of a deep-sea fish rhodopsin (15,16). Energy transfer from carotenoids or flavins to a retinal protein photoreceptor was suggested (17) to account for the well-structured action spectrum of phototaxis in the green alga *H. pluvialis* (18).

The discovery of xanthorhodopsin (10) provides evidence that efficient carotenoid-to-retinal energy transfer is indeed possible and can be utilized for transmembrane proton transport. Xanthorhodopsin, similar to bacteriorhodopsin, is a proton pump but also contains a carotenoid molecule, salinixanthin (19), with a light-harvesting function. It presents an opportunity to study excitation-energy transfer in a simple system with 1:1 chromophore stoichiometry.

Salinixanthin is a C_{40} carotenoid with 11 double bonds in the conjugated chain, one double bond in the ring, and a second in the keto group in the C4 position. On the other end, it has a glycoside and an acyl tail (Fig. 1). It was suggested to serve structural (membrane stabilization) and photoprotective roles (19,20), and as we show, in xanthorhodopsin it serves as a light-harvesting antenna. When bound to xanthorhodopsin, salinixanthin exhibits well-resolved vibronic absorption bands (10) and induced chirality (21), indicating less conformational heterogeneity than in the unbound state and an asymmetric conformation of the polyene chain and/or the ring. Changes of the retinal in the photochemical cycle and its removal by hydrolysis of the Schiff base strongly affect the absorption spectrum of the carotenoid (10). The tight and specific binding of the carotenoid has a functional rationale. Action spectra for proton transport (10,22), assayed directly and by photoinhibition of respiration in cells, showed that light absorbed by both retinal and salinixanthin is utilized for function. The involvement of carotenoid was suggested to be through excitation energy transfer to the retinal (10), as the latter can be expected to drive proton translocation in the way it does in the archaeal and eubacterial proton pumps, bacteriorhodopsin (11), archaerhodopsin (23), and proteorhodopsin (24), which are known to lack a carotenoid antenna but show substantial sequence homology to xanthorhodopsin (10,25).
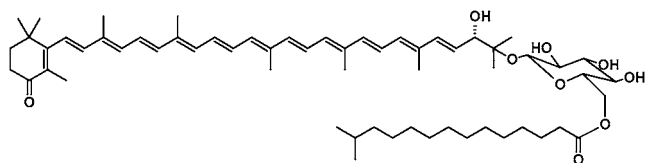
FIGURE 1 Chemical structure of salinixanthin. From Lutnaes et al. (19).

In this study, we present direct evidence for excitation energy transfer from the S_2 state of salinixanthin to the S_1 state of retinal in xanthorhodopsin. By detecting fluorescence from the S_1 state of retinal and the S_2 state of salinixanthin and measuring excitation spectra, we show that $45 \pm 5\%$ of the quanta absorbed by salinixanthin is transferred to the S_1 state of the retinal chromophore. From polarization anisotropy measurements, we determine the mutual orientation of the transition moments of salinixanthin and retinal. From spectra and quantum efficiency of carotenoid emission, we give a rough estimate for the distance between the centers of the two chromophores.

MATERIALS AND METHODS

Cultures of *Salinibacter ruber* strain M31 were grown as described earlier (10,26). Cell membranes containing xanthorhodopsin were obtained by lysing the cells with overnight dialysis against distilled water, subsequent washing in 100 mM NaCl and then in distilled water, and finally collecting by centrifugation (27). This procedure removed most other membrane proteins and excess salinixanthin, and, by fragmenting the membranes, it dramatically decreased light scattering.

The samples contained 20 mM buffer (MES for pH 5.5 and BICINE for pH 8). For retinal removal, hydrolysis of the retinal Schiff base with 100 mM hydroxylamine at pH 8 was used (10,21,27). Illumination of the sample at 550–650 nm substantially accelerated hydrolysis. Nearly all of the retinal oxime produced (>90%) could be removed by washing the membranes in the presence of bovine serum albumin (18 mg/mL). Another modification of xanthorhodopsin was the reduction of the retinal-lysine Schiff base C=N double bond to a single bond with sodium borohydride. Similarly to the observations with bacteriorhodopsin (28–30), this treatment kept the retinal in the binding site but caused a shift of the absorption maximum from ~560 nm to 360 nm. The reaction was performed at pH 8 under illumination at 550–650 nm for 1 h. Concentration of $NaBH_4$ was 5 mg/mL or less. Higher concentrations caused partial bleaching of the carotenoid.

Fluorescence measurements

Measurements were performed at 20°C on an SLM Aminco spectrofluorometer, equipped with an OLIS Instrument Control and Data Analysis system (Bogart, GA) and a cooled housing (model 4100/4900, Amherst Scientific, Landing, NJ) for the detector (Hamamatsu R955). The fluorescence spectra were corrected for the wavelength dependence of the sensitivity of the photomultiplier. A 300-W Cermax short arc xenon lamp (PE300BUV, Perkin Elmer Optoelectronix, Fremont, CA) powered by a power supply (ISS, Champaign, IL) was used as a source for the excitation light. The optical axes of the excitation and emission beams were at 90°. Both channels were equipped with polarizers, which could be set to different angles, including 0° (vertical), 90° (horizontal), and 54.7° (magic angle). The excitation spectra used for the comparisons with absorption spectra were recorded under the magic angle conditions (31). The bandwidth of the emission channel for measuring the spectra of fluorescence emission was 4 or 8 nm (in most cases), and the bandwidth of the excitation beam was 4 nm.

Long-pass filters were placed in front of the emission monochromator. A filter transmitting at $\lambda > 690$ nm was used for the retinal emission, sampled at 720 nm (with 32-nm bandwidth), and a filter with transmission at $\lambda > 550$ nm was used for the carotenoid emission at 565 nm (with 8-nm bandwidth). The wavelength dependence of the intensity of the excitation light, passed through a double monochromator, was determined with photon counters based on Rhodamine B and Nile Blue in triangular cuvettes and a dilute solution of a laser dye LDS-751 (Exciton, Dayton, OH) in ethanol (2×10^{-2} OD in a 4-mm path-length cells).

For the measurements of the excitation spectra for retinal emission, 4×4 and 2×10 mm (2-mm path for the excitation beam) stoppered quartz cells (Starna, Essex, UK) were used. Absorbance of the samples was between 0.25 and 0.3 at the 486-nm absorption maximum.

For fluorescence spectra measurements, the 4×4-mm stoppered quartz cells were used, minimizing reabsorption of fluorescence. Excitation spectra of carotenoid emission at 565 nm were recorded in the same cuvettes. Carotenoid emission in the 500- to 600-nm region overlaps with the absorption spectrum. The maximum absorbance in this range was below 0.3. Nevertheless, the fluorescence spectra were corrected for reabsorption using the simple equation for the inner filter effect (31) ($F_{cor} = F_{obs}/10^{-A/2}$, where A is the absorption spectrum). Typically, each spectrum was obtained as an average of 25 to 100 scans (depending on the signal/noise ratio), recorded with 1-nm steps and a 4-s integration time per step.

Correction of fluorescence spectra for Raman scattering from water and from the xanthorhodopsin chromophores

Raman scattering from water appears as a peak shifted ~3370 cm^{-1} from the excitation wavelength, corresponding to the O-H stretch vibration (in D_2O the peak shift from O-D stretch was ~2470 cm^{-1}). With some wavelengths of excitation, this Raman scattering was evident in the excitation and emission spectra. When retinal emission was sampled at 720 nm, the contribution from Raman scattering was relatively small (a very weak band at 580 nm). However, in the 500- to 600-nm range, the contribution from Raman scattering was comparable in magnitude to the vibronic bands of carotenoid fluorescence and had to be subtracted. The emission from a 4×4 mm cuvette with buffer only (20 mM MES or BICINE) was therefore measured under the same conditions as the sample. The amplitude of the Raman band in the sample is lower than that in buffer by a factor T_c, which takes into account the lower intensity of the excitation beam from absorption of the exciting light and reabsorption of the Raman emission by xanthorhodopsin (31). $T_c = 10^{-(A(\lambda ex)+A(\lambda sc)/2)}$, where $A(\lambda_{ex})$ is absorbance at the excitation wavelength and $A(\lambda_{sc})$ is absorbance at the maximum of the Raman band. In addition to the subtraction, it was helpful to use D_2O, instead of H_2O to shift the Raman band away from the overlapping fluorescence band.

Variation of the excitation wavelength by 5 nm was used to detect and remove the contribution from the chromophore Raman bands. The Raman bands most likely originate from the C=C and C–C stretch of the conjugated chains of the carotenoid and the retinal (32). At least two bands that shift with the shift of excitation wavelength, by 1450 and 1090 cm^{-1}, were superimposed on the authentic 529-, 564-, and 605-nm fluorescence bands of salinixanthin. By using excitation at 450–470 nm we could avoid contribution from these Raman lines to the fluorescence spectrum at $\lambda > 510$ nm.

Estimation of the quantum efficiency of antenna carotenoid fluorescence

Excitation in the 450- to 470-nm range produced fluorescence spectra containing two well-resolved bands at 529 and 564 nm and a weaker band at 600–605 nm. The spectrum was fitted with the sum of Gaussians. The intensity of this emission (expressed as the integral of the three bands, $I_{bCar} = 0.28$ relative units) was compared with the intensity of fluorescein fluorescence. A highly diluted solution of fluorescein in ethanol ($A = 8.1 \times 10^{-3}$ OD in a 4×4-mm cuvette) was used. Because the quantum efficiency of

fluorescein is very high ($\phi_{fl} \approx 0.95$), the intensity of the excitation beam was decreased by three orders of magnitude, using a 6-mm-thick neutral-density filter ($T = 0.00134$ at 460 nm) to use the same measurement conditions as for carotenoid fluorescence. The integral under the fluorescence band of fluorescein (I_{fl}) was 1.024 relative units. From these values, the quantum efficiency of the bound (antenna) carotenoid emission was calculated as the ratio:

$$\phi_{bCar} = \phi_{fl} I_{bCar}(1 - T_{fl})T/I_{fl}(1 - T_{bCar}) = 3.1 \times 10^{-5} \quad (1)$$

The fraction of light absorbed by the antenna carotenoid at 460 nm ($1 - T_{bCar}$) was calculated from the absorption spectrum, taking into account the absorbance of retinal at 460 nm and absorbance of nonbound carotenoid (17% of total carotenoid) present in the sample.

It is likely that the sum of three Gaussians used in this estimate to approximate the carotenoid fluorescence spectrum underestimates the total emission by ~25–30%, as one can conclude from comparison of the experimental and theoretical spectra. With this correction, the quantum efficiency of carotenoid fluorescence was inferred to be $\phi_{bCar} = 4 \times 10^{-5}$.

Estimation of the excited state (S_2) lifetime of antenna carotenoid

The rate constant for fluorescence from the S_2 excited state of salinixanthin (k_f) was estimated from the Strickler-Berg (33) relation:

$$k_f = 2.88 \times 10^{-9} n^2$$
$$\times \left(\int F(\nu)d\nu \Big/ \int \nu^{-3}F(\nu)d\nu \right) \times \int \nu^{-1}\varepsilon(\nu)d\nu, \quad (2)$$

where $F(\nu)$ is the fluorescence spectrum of bound salinixanthin. It was approximated by the sum of three Gaussian bands plotted against the wavenumber. The absorption spectrum of the antenna carotenoid was taken from deconvolution of the absorption and excitation spectra. The extinction coefficient for salinixanthin ε has not been determined exactly (S. Liaaen-Jensen, personal communication), but the best estimate is that it is in the range of 130,000–150,000 M^{-1} cm^{-1}. The refractive index n for the membranes was taken as 1.45, as for purple membranes (34,35). Integration of the absorption and fluorescence bands yields 1.2–1.4 ns for the natural lifetime ($\tau_f = 1/k_f$, smaller value for the larger extinction). The actual lifetime of S_2, τ, was calculated as a product of τ_f and the quantum yield of fluorescence, $\phi_f = (4 \pm 2) \times 10^{-5}$. The value of τ thus obtained is in the 70 ± 30 fs range.

Fluorescence excitation anisotropy spectrum $R(\lambda)$

The $R(\lambda)$ spectrum was used to obtain information on the mutual orientation of the carotenoid antenna and retinal chromophore. It was calculated from the excitation spectra measured under parallel and perpendicular polarization of the exciting and emission beams, I_{vv} and I_{vh} (the first subscript stands for the polarization of the excitation beam, the second for the polarization of emission beam). Correction for different transmission of vertically and horizontally polarized light through the emission monochromator was done by measuring the ratio of fluorescence intensities under horizontal excitation (I_{hh}/I_{hv}) (31). The fluorescence intensity was measured at 720 nm ($\Delta\lambda_{1/2} = 32$ nm). For the 720-nm emission, the (I_{hh}/I_{hv}) ratio was constant and equal to 3.5. The fluorescence anisotropy $R(\lambda)$ was calculated as $R = (i - 1)/(i + 2)$, where $i = (I_{vv}/I_{vh})(I_{hh}/I_{hv}) = 3.5 (I_{vv}/I_{vh})$. To check the accuracy of the anisotropy spectrum $R(\lambda)$, it was measured also on a different fluorometer, PC-1 (ISS) at the Fluorescence Dynamics Lab (University of California, Irvine), equipped with photon-counting detector. The results were similar.

The excitation anisotropy spectrum for the emission of retinal chromophore of xanthorhodopsin was fit to a sum of two terms:

$$R = f_r R_r + f_c R_c \varphi_m, \quad (3)$$

where R_r and R_c are the anisotropies of retinal and carotenoid (both essayed through the retinal emission), f_i is fractional absorption of each component

($f_r = A_r/(A_r + A_{bCar})$; $f_c = 1 - f_r$) and φ_m is the efficiency of energy transfer. The angle between the transition dipole moments of the carotenoid absorption and retinal emission, β_{cr}, was calculated from the formula for fundamental anisotropy of a fluorophore (31):

$$R_c = 0.2 \left(3\cos^2\beta_{cr} - 1\right). \quad (4)$$

Bacteriorhodopsin was used in this study for comparison of its fluorescence, excitation, and anisotropy spectrum and fluorescence quantum yield with those of xanthorhodopsin.
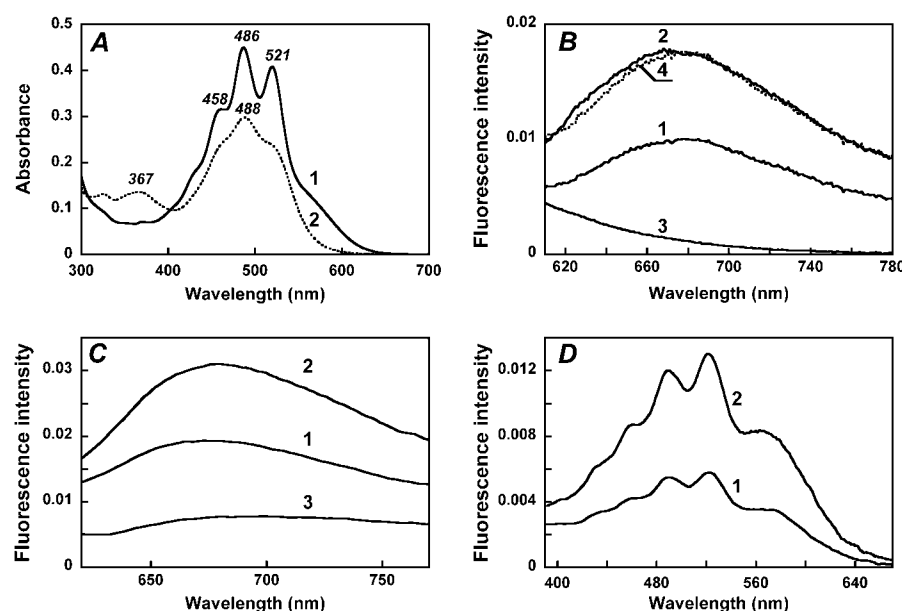
RESULTS

Fluorescence of the retinal chromophore of xanthorhodopsin

In xanthorhodopsin, the absorption bands of carotenoid are sharp peaks at 521, 486, and 458 nm, and the broader band of the retinal chromophore appears as a shoulder at ~560 nm (Fig. 2 *A*, *spectrum 1*). Excitation at 560 nm, where the absorbance of the bound salinixanthin is negligible, produces a fluorescence emission band with a maximum at ~685 nm (Fig. 2 *B*, *spectrum 1*). As in bacteriorhodopsin (36–40), this retinal fluorescence is a broad band extending into the infrared. It exhibits a large Stokes shift of ~3200 cm^{-1}. As expected, removal of the retinal with hydroxylamine eliminates the retinal fluorescence band (Fig. 2 *B*, *spectrum 3*).

The quantum yield of fluorescence is of the order of 5×10^{-4}, and depends on pH. The latter affects the environment of the retinal chromophore through protonation of the Schiff base counterion ($pK_a = 6.4$ in the membranes used). The fluorescence spectra at pH 5.5 and pH 8.0, i.e., below and above the pK_a of the retinal Schiff base counterion of xanthorhodopsin, are shown in Fig. 2 *C*, along with the spectrum for bacteriorhodopsin. The fluorescence quantum yield at pH 8 was ~2.5-fold lower than that at pH 5.5 (Fig. 2 *C*, *spectra 1* and *2*) and ~3-fold higher than that in bacteriorhodopsin under similar excitation conditions (Fig. 2 *C*, *spectrum 3*). At pH 8, the counterion aspartate in xanthorhodopsin is deprotonated, and the absorption maximum of the retinal is 3–5 nm blue-shifted (41) from its position at ~563 nm at pH 5.5. The maximum in the fluorescence spectrum also does not change substantially between pH 5 and 8. The effects of the neutralization of the counterion, by protonation or residue replacement, on the lifetime of the excited state and the fluorescence intensity were observed earlier in bacteriorhodopsin (39,42,43). In the latter, protonation of the counterion causes a significantly larger increase in the retinal chromophore fluorescence quantum yield compared with that in xanthorhodopsin (>10-fold versus 2.5-fold). The quantum efficiency of the retinal chromophore fluorescence of xanthorhodopsin is ~7×10^{-4} at pH 5.5 and 3×10^{-4} at pH 8 (assuming that the yield for bacteriorhodopsin fluorescence is 10^{-4} (36,39)).

Excitation spectrum for retinal emission: evidence for the excitation energy transfer

The most direct evidence for energy transfer in the excited state is fluorescence emission from the acceptor when the

FIGURE 2 Absorption, fluorescence, and excitation spectra of xanthorhodopsin. Effect of retinal removal with hydroxylamine. (A) Absorption spectrum of cell membranes of *Salinibacter ruber* containing xanthorhodopsin (at pH 5.5) before (*spectrum 1*) and after (*spectrum 2*) hydrolysis of the retinal Schiff base with hydroxylamine. The treatment converts the covalently bound retinal to the retinal oxime, whose absorption maximum is shifted from 563 nm to 367 nm, and the sharp carotenoid vibronic bands broaden. (B) Fluorescence emission of xanthorhodopsin, pH 5.5, excitation at 560 nm (*spectrum 1*) and 520 nm (*spectrum 2*). Spectrum 3, after hydroxylamine treatment and removal of the retinal oxime, excitation at 560 nm. Spectrum 4, spectrum 1 normalized to the amplitude for 520 nm excitation, by multiplying by 1.7. (C) Comparison of the xanthorhodopsin fluorescence bands at pH 8 (*spectrum 1*) and pH 5.5 (*spectrum 2*) with that of bacteriorhodopsin, pH 6 (*spectrum 3*). Excitation: 560 nm, 8 nm bandwidth. Absorbances of the samples at 560 nm were 0.29, 0.32, and 0.33, respectively. A small contribution from the Raman scattering of water was subtracted. (D) Fluorescence excitation spectra for the emission of xanthorhodopsin, sampled at 720 nm, at pH 8 (*spectrum 1*) and pH 5.5 (*spectrum 2*). Excitation beam bandwidth 4 nm.

donor is excited. Excitation at 520 nm, where both retinal and carotenoid absorb, produces a similar emission band but with ~1.7-fold higher amplitude at the same exciting intensity (Fig. 2 B, *spectrum 2*). Thus, excitation of the carotenoid enhances emission by the retinal, providing evidence for energy transfer. When scaled together, the emission spectra from 520-nm and 560-nm excitation are almost coincident at $\lambda > 680$ nm (Fig. 2 B, *spectra 2* and *4*), indicating that direct emission from the carotenoid and Raman scattering do not contribute significantly at these wavelengths.

The efficiency of different excitation wavelengths in generating retinal emission (the excitation spectrum) was measured for pH 5.5 and 8 (Fig. 2 D). Although the fluorescence is from retinal (sampled at 720 nm), both excitation spectra exhibit, in addition to the expected 560-nm band of the retinal chromophore, sharp carotenoid bands at 521, 486, and 458 nm. These bands indicate that excitation energy from light absorption by the carotenoid in the S_o to S_2 transition is transferred to the excited singlet state of retinal, S_1, and contributes to emission from this state. Within the accuracy afforded by the lower signal/noise, the excitation spectrum at pH 8 exhibits similar shape but smaller amplitude than the one at lower pH (from the lower quantum yield of the retinal chromophore emission at the higher pH). The similarity of the excitation spectral shape at high and low pH indicates that contribution of the carotenoid bands to the excitation is through energy transfer to the retinal and that the efficiency of transfer is about the same at high and low pH (an accurate estimate of efficiency is made below). If there is a contribution to the retinal fluorescence at 720 nm from carotenoid emission, being pH independent, it is small.

The excitation spectrum for retinal emission is similar to the action spectra for proton transport (10) and photoinhibition of respiration in *Salinibacter ruber* (22). This provides evidence that involvement of carotenoid in these processes is through excitation energy transfer to the S_1 singlet state of retinal.

Fluorescence of salinixanthin in xanthorhodopsin

Excitation at wavelengths where the carotenoid absorbs produces additional low-intensity fluorescence bands at 529, 564, and 600–605 nm. They were dissected from the underlying light scattering by deconvolution of the spectrum into Gaussians (Fig. 3 A). The bands did not change position when the excitation was at different wavelengths between 450 and 500 nm and thus can be distinguished from the Raman bands, which shift with excitation wavelength (Fig. 3 B). After hydroxylamine treatment, the fluorescence band becomes broader and loses its structure, similarly to the broadening of the absorption band of the carotenoid (Fig. 3 A, *spectrum 6*, and Fig. 2 A, *spectrum 2*). The excitation spectrum for the 565-nm band exhibits maxima at 521, 486, and 456 nm (data not shown). The well-resolved emission bands at 528–530 and 564 nm are in the wavelength range expected for fluorescence from the S_2 excited state of salinixanthin. Emission from the S_2 level has been observed earlier for a number of purified carotenoids with long conjugated chains ($n > 9$) in organic solvents (reviewed by Frank and Cogdell (44)). Its typical features are a very small Stokes shift (only 150–300 cm^{-1}) between the short-wavelength fluorescence band and the long-wavelength absorption maximum and nearly perfect mirror
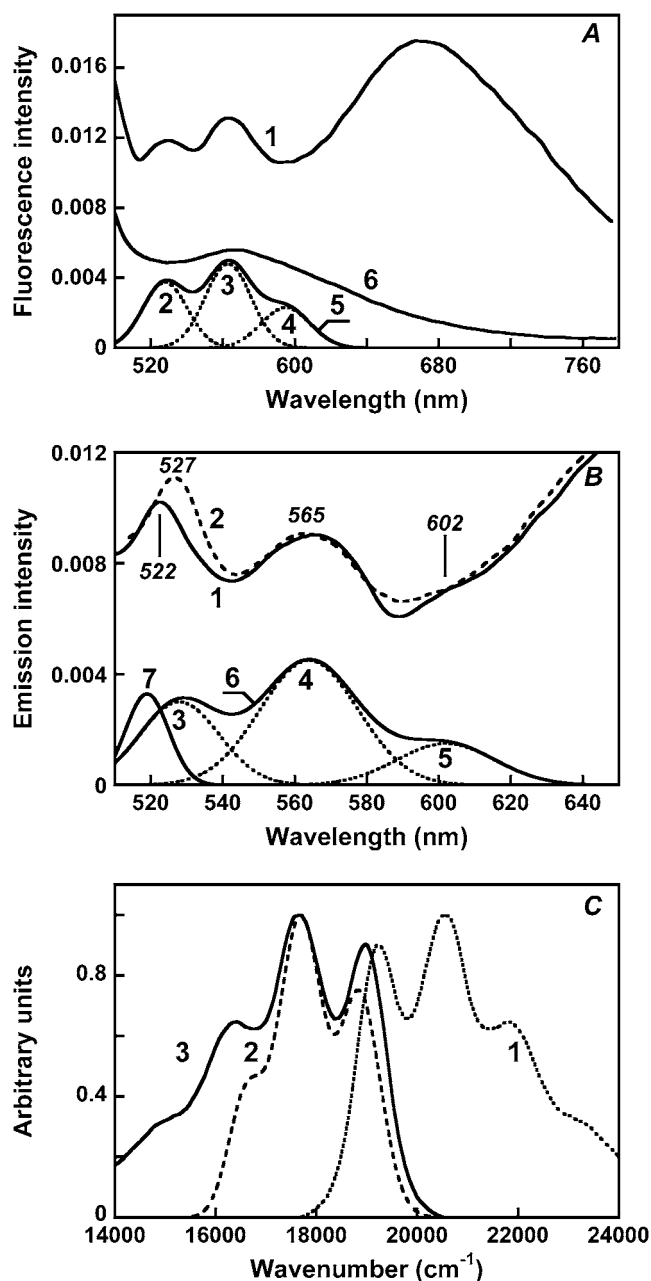
FIGURE 3 Fluorescence of salinixanthin chromophore of xanthorhodopsin. (*A*) Fluorescence emission of xanthorhodopsin, excitation at 470 nm. Spectrum 1, measured emission; curves 2–4, Gaussian fits to three short-wavelength peaks. The residual contains mostly light scattering, and is not shown. Spectrum 5, sum of bands 2–4 (estimated emission from salinixanthin). Spectrum 6, measured emission as for spectrum 1, but after hydroxylamine bleaching, which removes the retinal and broadens the carotenoid peaks (see Fig. 2 *A*, *spectrum 2*). (*B*) Correction of fluorescence spectra for the contribution of xanthorhodopsin Raman band by deconvolution into Gaussian bands. Spectra 1 and 2 (*dashed*), measured emission spectra of *S. ruber* membranes in 20 mM MES, pH 5.5, produced by excitation at 485 and 490 nm, respectively. Note the shift of the sharp band at 522 nm in spectrum 1 to 527 nm in spectrum 2. Spectra 3–7, deconvoluted component spectra. Bands 3–5, Gaussians that fit the fluorescence bands of salinixanthin in xanthorhodopsin (maxima at 528, 563, and 602 nm, bandwidths, 26, 32, and 32 nm, and relative amplitudes 0.003, 0.0045, and 0.0015, respectively); spectrum 6, sum of the three Gaussian bands (*spectra 3–5*), assumed to be the carotenoid

symmetry of the fluorescence and absorption spectra (6). As shown in Fig. 3 *C*, the fluorescence bands of salinixanthin share these features. The Stokes shift between the 521-nm absorption and 529-nm emission bands is 290 cm^{-1}. The experimental fluorescence spectrum is very similar to the expected mirror image, particularly in the main maxima. Based on this, we assign the well-resolved emission bands at 529 and 564 nm to fluorescence from S_2. As comparison of the experimental and predicted spectra shown in Fig. 3 *C* indicates, we were unable to resolve the long-wavelength part of the spectrum because of overlap with the broad retinal emission.

Carotenoids with long chains of conjugated bonds, in organic solvents, typically show such emission from the S_2 level (6,44,45). Emission from S_1 of salinixanthin would be expected at $\lambda > 720$ nm (6), and for carotenoids with long polyene chains, such as salinixanthin, its quantum efficiency should be considerably lower than that of S_2 emission because it is an optically forbidden "dark" state (6,46,47). No signs of S_1 carotenoid emission were detected in this study.

The salinixanthin fluorescence emission spectrum with a maximum at 564 nm overlaps the absorption spectrum of the retinal chromophore ideally, as expected for a well-matched donor-acceptor pair. The quantum efficiency of carotenoid fluorescence is ca. 4×10^{-5}. The very low quantum efficiency of the antenna carotenoid emission agrees well with data for carotenoids with long chains ($n = 10, 11$) in organic solvents, which exhibit emission from the S_2 level with quantum efficiency in the range of $2 \times 10^{-5} - 10^{-4}$ (reviewed by Polivka and Sundström (6) and Frank and Cogdell (44)).

From the absorption spectrum of salinixanthin and its fluorescence quantum yield, the lifetime of S_2 is estimated to be very short, 70 ± 30 fs. Yet, from analogy with similar carotenoids, the S_1 state of salinixanthin should be at a far lower level than S_1 of the retinal, which would exclude its participation in energy transfer. Can energy transfer to the retinal take place from S_2? Direct evidence for such energy transfer was obtained in experiments with borohydride reduction of the Schiff base.

Energy transfer occurs from the S_2 level of the carotenoid: evidence from the effect of reduction of the retinal Schiff base on the salinixanthin fluorescence intensity

Reduction of the Schiff base with borohydride shifts the retinal absorption band from 560 nm to 360 nm (Fig. 4 *A*).
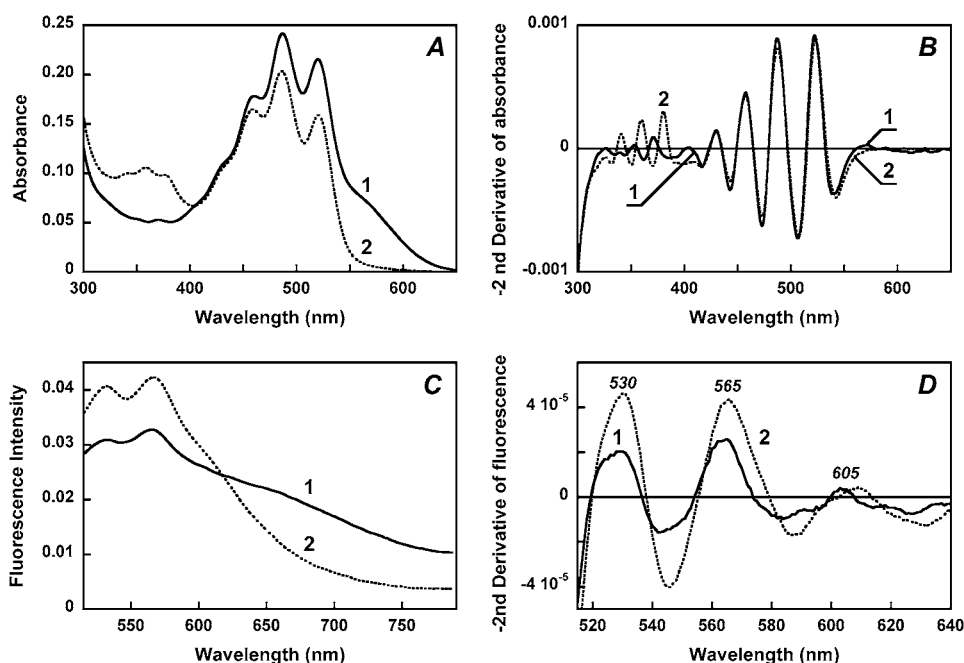
FIGURE 4 Effect of reduction of the retinal Schiff base with sodium borohydride on the absorption spectrum of xanthorhodopsin and the fluorescence intensity of salinixanthin. (A) Absorption spectra of (1) cell membrane fraction containing xanthorhodopsin, pH 8.5, 100 mM NaCl; (2) after reduction of the retinal Schiff base with sodium borohydride. (B) Second derivatives of the spectra in panel A (multiplied by −1) showing that the sharp carotenoid bands at 521, 486, and 456 nm did not change their shape on retinal Schiff base reduction. (C) Fluorescence spectra: (1) initial, pH 8.5; 2, treated with NaBH$_4$. (D) Second derivatives (multiplied by −1) of the fluorescence spectra of: (1) initial sample; (2) after treatment with NaBH$_4$. The maxima correspond to salinixanthin fluorescence bands.

The retinylidene chromophore is now bound through a single bond to the protein and remains in its binding site as follows from the well-resolved bands 345, 360, and 378 nm from the planarized ring-chain retinal conformation, as observed also for bacteriorhodopsin (30). Most important, the reduction of the Schiff base linkage did not significantly affect the binding of the carotenoid. It exhibits the same well-resolved bands as in the native pigment (Fig. 4 A, spectrum 2, and Fig. 4 B) with only slight decrease in their amplitude (<15%). This indicates that retinal ring and/or chain controls the conformation of the carotenoid, consistent with the results obtained in studies with retinal analogs and retinol, which indicate that the functional conformation of salinixanthin is produced by the entry of the retinal into its binding site, before formation of the Schiff base (27).

The sample with the reduced retinylidene provides an opportunity to test directly whether energy transfer occurs from the same excited state level(s) that produce the fluorescence emission. The shift of the retinal band to 360 nm eliminates energy transfer from carotenoid to retinal by elevating the excited state level of the latter far above that of the donor. This should result in an increase in fluorescence quantum efficiency of the donor because it is determined by the ratio of rate constant of fluorescence (k_f), thermal dissipation (k_d), and energy migration (k_m), $\phi_f = k_f/(k_f + k_d + k_m)$.

Comparison of the fluorescence emission before and after borohydride reduction shows the expected disappearance of the retinal chromophore emission band (Fig. 4 C) and an increase in the emission intensity in the region of carotenoid emission. Sharp bands from this emission at 530 and 565 nm are present in the difference spectrum, curve 2 minus curve

1 (not shown). To quantify the amplitude of these bands, the second derivative of the fluorescence spectra was taken (Fig. 4 D). This separated the sharp bands from the broad background emission, which originates, as expected, from the reduced retinylidene chromophore (despite excitation at wavelengths far from its absorption band). The second derivatives of the fluorescence spectra of the initial sample and after NaBH$_4$ reduction show sharp bands at 530, 565, and 605 nm and an approximately twofold increase in intensity of these bands in the sample with the acceptor missing (after NaBH$_4$ reduction). This result is consistent with energy transfer being in direct competition with emission from S$_2$ and implies that in the native xanthorhodopsin the rate constants for the energy transfer and internal conversion are approximately equal. Thus, the efficiency of energy transfer is near 50%. A more precise estimate was obtained from excitation spectrum of retinal fluorescence.

Efficiency of excitation energy transfer

Fig. 5 A compares the absorption spectrum of xanthorhodopsin (spectrum 1) with the excitation spectrum for 720-nm emission (spectrum 2). The efficiency of energy transfer can be estimated from comparing the contributions of the carotenoid and retinal to the excitation spectrum at magic-angle conditions, with those in the absorption spectrum. To do this, the individual spectra of the salinixanthin and retinal chromophores (Fig. 5 B) were obtained by deconvolution of the spectra in Fig. 6 A and used to fit the absorption and excitation spectra.

In this calculation, correction had to be made for the presence of a small fraction of the carotenoid not bound to
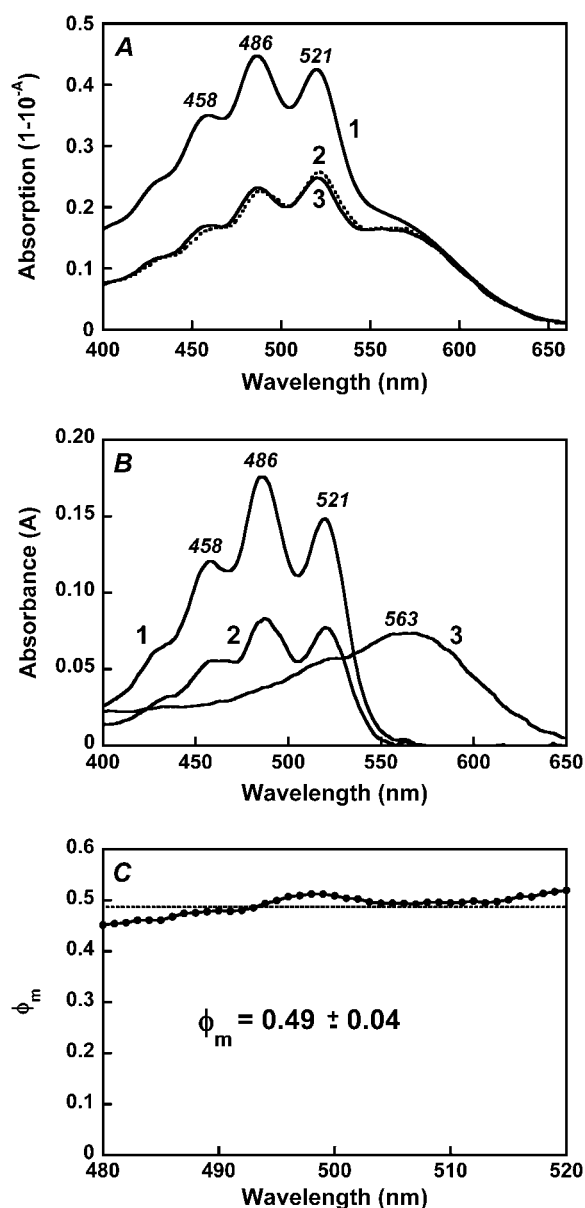
FIGURE 5 Fluorescence excitation spectra of the retinal chromophore: comparison with absorption spectra and estimation of the efficiency of energy transfer. (*A*) Spectrum 1, absorption spectrum of xanthorhodopsin, pH 5.5. Spectrum 2, excitation spectrum for emission at 720 nm measured at magic angle (excitation with vertically polarized light (0°) and emission measured with polarizer set at 54.7°, which eliminates effects from preferential excitation). Excitation bandwidth 4 nm, emission bandwidth 32 nm. Spectrum 3, best fit of the excitation spectrum with retinal and carotenoid components in the absorption spectrum and with an efficiency for energy transfer of 0.49, determined as described in the text. (*B*) Spectra of the components of the excitation and absorption spectra: (*1*) carotenoid component in the absorption spectrum after subtraction of the retinal component and nonbound carotenoid; (*2*) carotenoid component in the excitation spectrum; (*3*) retinal component in the absorption and excitation spectra. (*C*) The ratio of the spectra of carotenoid components in the excitation and absorption spectra (*spectrum 2* divided by *spectrum 1* in Fig. 5 *B*). This ratio is the quantum efficiency of energy transfer, ϕ_m, from the carotenoid to the retinal.
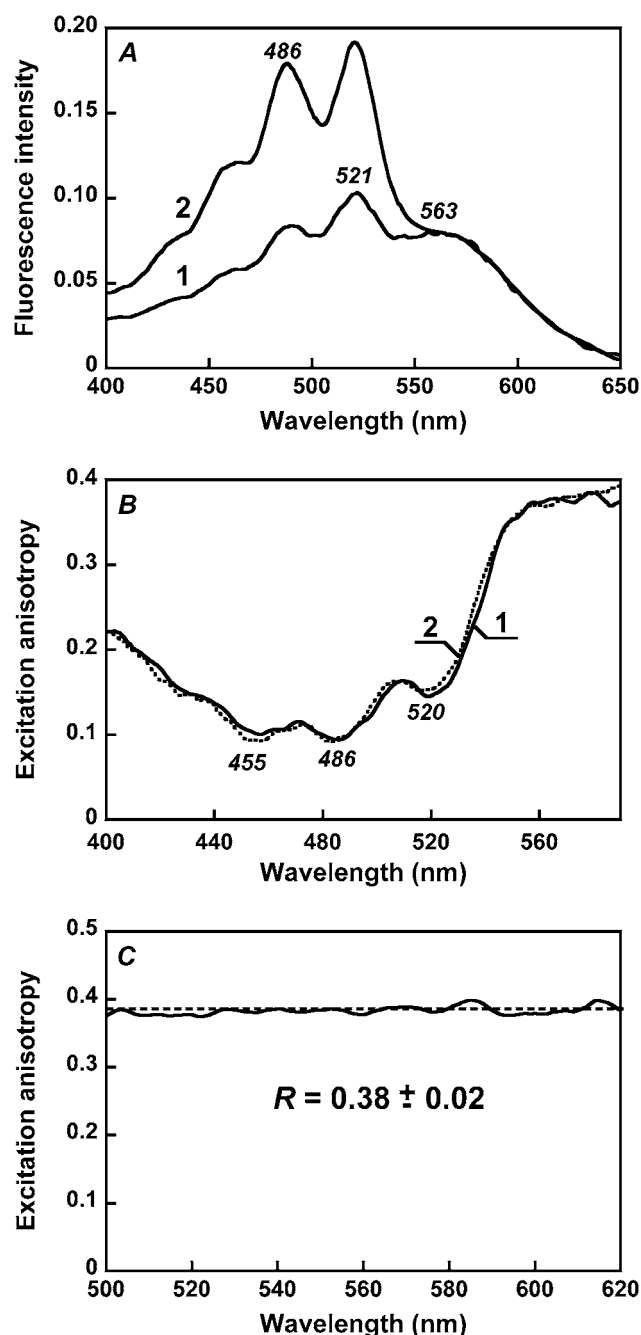
FIGURE 6 Anisotropy of the excitation of retinal fluorescence. (*A*) Fluorescence excitation spectra (for 720-nm emission) measured under parallel and perpendicular polarization of excitation and emission beams. Spectrum 1, both beams vertically polarized (I_{vv}); spectrum 2, the polarizer in the emission beam set horizontally (I_{vh}). The first and second subscripts stand for polarization of the excitation and emission beams, respectively. (*B*) Spectrum of excitation anisotropy, $R(\lambda)$, and its fit as a sum of two components, from retinal and carotenoid. Spectrum 1, excitation anisotropy; spectrum 2, fit of the anisotropy by the sum of two components, from the retinal and the carotenoid in xanthorhodopsin, R_r and R_{bCar}, multiplied by the fractional absorbances of the two chromophores and the quantum efficiency of energy transfer (for the carotenoid), $R(\lambda) = R_r f_r(\lambda) + R_{bCar} f_{bCar}(\lambda)\phi_m$. From the fit, the anisotropies for the retinal and carotenoid components were determined to be $R_r = 0.38$, $R_{bCar} = -0.04$, respectively. (*C*) Fluorescence excitation anisotropy of bacteriorhodopsin. Dashed line is fit of experimental data with a constant, equal to 0.38.

xanthorhodopsin, which will affect the carotenoid/retinal ratio in the absorption spectrum and produce some screening effect as well. The spectrum of nonbound carotenoid has a broader vibronic structure (Fig. 2 A, *spectrum 2*) (10,21), and its contribution broadens somewhat the vibronic bands of the absorption spectrum as compared with the excitation spectrum. The fraction of excess, nonbound, carotenoid could be determined from comparison of absorption and excitation spectrum at wavelengths ~560 nm, where bound carotenoid does not absorb and all the difference between the two spectra is caused by the presence of nonbound carotenoid. From these considerations, the fraction of excess carotenoid in these membranes was determined to be 17 ± 3%.

The efficiency of energy transfer was estimated by fitting the data to the equations:

$$Ex(\lambda) = (1 - T) \times (A_r + \phi_m A_{bCar})/A \quad (5)$$

$$A = A_r + A_{bCar} + A_{nbCar}, \quad (6)$$

where $Ex(\lambda)$ is the experimental excitation spectrum, A and T are the absorbance and transmission spectra of the sample ($T = 10^{-A}$), ϕ_m is the quantum efficiency of energy transfer, A_{bCar} the absorption spectrum of carotenoid bound to xanthorhodopsin, A_{nbCar} the absorption spectrum of the excess, nonbound carotenoid, and A_r is the absorption spectrum of the retinal component of xanthorhodopsin. The spectrum A_r (Fig. 5 B, *spectrum 3*) was taken from deconvolution of the excitation spectra measured under different polarization conditions shown in Fig. 6 A. It is similar to the spectrum of bacteriorhodopsin shifted 5 nm toward shorter wavelengths, but with a small shoulder at 510–515 nm. The spectrum of nonbound carotenoid was taken from the spectrum after hydroxylamine treatment (Fig. 2 A, *spectrum 2*). The deconvolution of the absorption and excitation spectra and estimation of quantum efficiency of energy transfer (as the ratio of the bound carotenoid component in the excitation and absorption spectra, normalized in the retinal band) are shown in Fig. 5, B and C. The ratio of carotenoid contributions yields a fairly constant value for the efficiency for energy transfer across the wavelength range considered, equal to 49 ± 4%. This value is somewhat higher than the previously estimated 40% from measurements of proton transfer in vesicles and photoinhibition of respiration in intact cells (10), mainly because the fluorescence excitation spectra allowed more precise analysis and a better estimate of the fraction of nonbound carotenoid (the action spectrum obtained earlier for transport function and the fluorescence excitation spectrum are very similar). Another factor is a possible, but minor, contribution of the carotenoid S_2 emission to the measured emission at 720 nm. If the true spectrum of carotenoid S_2 emission follows the theoretical curve in Fig. 3 C, the contribution from S_2 emission can be estimated as <5% of total emission when excitation is at 470–485 nm. This possible contribution would decrease the quantum efficiency of energy transfer by a few percent, to ~45 ± 5%.

Excitation anisotropy and mutual orientation of the two chromophores

The shape of the excitation spectrum depends strongly on polarization of the excitation and emission beams. When both beams are vertically polarized, the retinal component dominates, but when emission is measured with horizontal polarization, the carotenoid component does (Fig. 6 A, *spectra 2* and *1*, respectively). This indicates that the two chromophores are not parallel. The angle between the transition dipole moments of the carotenoid and retinal was estimated from the fluorescence excitation anisotropy spectrum, $R(\lambda)$, (Fig. 6 B). At >580 nm, where only the retinal chromophore absorbs, the anisotropy is 0.38, i.e., near the theoretical value of 0.4 when the transition dipole moments in absorption and emission have the same orientation. This is as expected because rotation of the protein in the membrane fragments is much slower than the excited state lifetime, and apparently relaxation of the retinal in the excited state does not involve large changes in the orientation of the transition dipole moment. Indeed, in bacteriorhodopsin, $R(\lambda)$ is a constant 0.38 ± 0.02 within its main absorption band (Fig. 6 C), in agreement with earlier measurements by Kouyama et al. (42). From the hexagonal symmetry of monomers in purple membranes, the angle between the retinal transition moments in a trimer (48) is 120°. If energy transfer among the three retinals in the trimer took place, it would cause a decrease of anisotropy. The observed constant anisotropy in Fig. 6 C, at its theoretical high limit, is in agreement with the suggested lack of energy transfer between the retinal chromophores of monomers within the bacteriorhodopsin trimer (37,39,49).

In xanthorhodopsin, at wavelengths where absorption of the carotenoid dominates, the anisotropy decreases to ~0.1 (minima at 486 and 520 nm). The total anisotropy is the sum of the two components, from the carotenoid (R_c) and retinal (R_r), each multiplied by their respective contributions. From the fit of the calculated spectrum to the experimental anisotropy spectrum (Fig. 6 B, *spectra 1* and *2*), R_c is −0.04. The dependence of the anisotropy on the angle θ between the transition moments of absorption (by the carotenoid) and emission (by the retinal) is $R = 0.2 (3\cos^2\theta - 1)$. From this relation, the angle between the transition moments of the $S_0 \rightarrow S_2$ carotenoid absorption and $S_1 \rightarrow S_0$ retinal emission is 59°. The average of four measurements is 56° ± 3°.

DISCUSSION

Energy transfer pathway and efficiency

The results of the present fluorescence study confirm the suggestion that carotenoid involvement in light-induced proton transport in xanthorhodopsin is through excitation energy transfer to retinal. The efficiency of energy transfer, 45 ± 5%, is similar to our initial estimate from the action spectra for proton pumping, ~40% (10).

The increase in the intensity of the very weak fluorescence bands of salinixanthin at 530 and 565 nm on reduction of the retinal Schiff base linkage with borohydride indicates that energy transfer occurs from the S_2 level of the antenna carotenoid, as depicted in Fig. 7. The extremely low quantum efficiency of salinixanthin fluorescence in xanthorhodopsin indicates further that the lifetime of the excited state is 100 fs or less and that energy transfer should occur rapidly enough to compete with internal conversion, with a time constant of ~200 fs. These estimates from the steady-state fluorescence studies are in agreement with femtosecond absorption measurements (T. Polivka, S. P. Balashov, P. Chabera, A. Yartsev, V. Sundstrom, E. S. Imasheva, and J. K. Lanyi, unpublished data). This rate is comparable to the rates of energy transfer from carotenoids S_2 ($1B_u^+$) states to Q_x state of bacteriochlorophyll in light-harvesting complexes of photosynthetic bacteria (6,50). In the latter, the Q_y band of the bacteriochlorophyll is below the S_1 level of the carotenoid. This long-lived state is populated in the process of internal conversion from S_2 and, together with the intermediate dark state ($1^1B_u^-$), serves as an alternative pathway for energy transfer that is efficient in shorter polyenes but ceases in carotenoids with $n > 11$ (50,51). In xanthorhodopsin the S_1 level of salinixanthin is expected to be considerably lower than the S_1 excited state of retinal and cannot take part in energy transfer. The intermediate "dark" ($1^1B_u^-$) level of salinixanthin could be at > 630 nm (estimated using formula from Furuichi et al. (52)), i.e., below the retinal chromophore absorption. This makes questionable any significant contribution of this state in energy transfer. The S_2 ($1^1B_u^+$) state of salinixanthin is the major donor of excitation for the retinal chromophore. A similar conclusion on the predominant role of the S_2 state in energy transfer from β-carotene to chlorophyll was reached for photosystems I and II (53).

Similar to the carotenoid, all-*trans*-retinal exhibits several excited states (54–56). Their order depends on the environment. In bacteriorhodopsin and other retinal proteins where retinal is bound via a protonated Schiff base to a lysine, the lowest excited singlet π,π^* state (S_1) is a strongly allowed $1B_u^+$ state characterized by a large oscillator strength and large transition dipole moment (57). In bacteriorhodopsin it is responsible for a broad intense absorption band with maximum at 568 nm. Approximately 3500 cm^{-1} above the S_1 state there is a "forbidden" $2A_g^-$-like state (labeled as S_2 on the scheme), which was detected in bacteriorhodopsin in two-photon double resonance absorption spectra as a band at 488 nm (57). In free retinal the order of these states is the opposite: the A_g^--like state is lower than $1B_u^+$ (55,56). In the region of β-bands a third excited state (A_g^+-like) is located. It is sensitive to the configuration of retinal and is more pronounced in 11-*cis* isomers as a "*cis*" peak (57).

From the similar structure of the binding site (protonated Schiff base with a counterion), it is reasonable to assume that xanthorhodopsin has a similar order of excited states as bacteriorhodopsin, $1B_u^+$ being the lowest. This state must be the acceptor of the excitation energy from the carotenoid. The S_2 state is not accessible under one-photon excitation; it is expected to have energy corresponding to the 480 nm light, which is above the 0-0 transition of the carotenoid, and it is unlikely that it plays a significant role as an energy acceptor. However, it might be involved in the subsequent photoisomerization that occurs after transition out of the photochemically inactive Franck-Condon region (sometimes called the H state) to the region of the S_1 excited state called I (58,59) (or fluorescing state), also of $1B_u^+$ electronic configuration. The transition to the I state apparently involves relaxing of the conjugated chain and particularly the
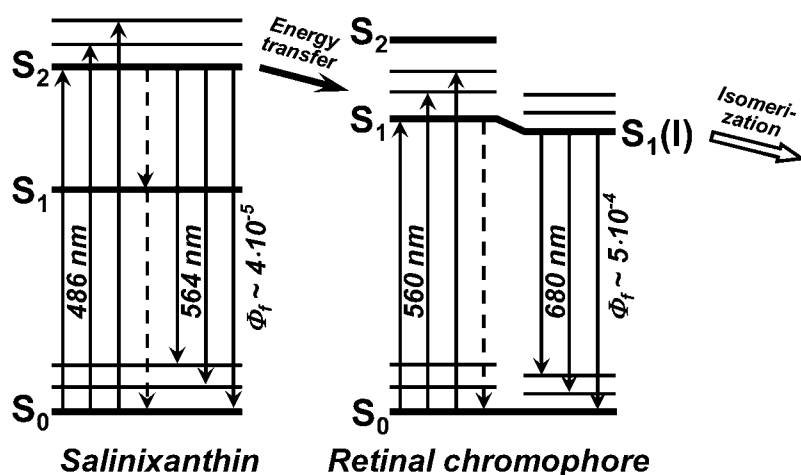

FIGURE 7 Suggested scheme of energy transfer pathway from salinixanthin to the retinal chromophore of xanthorhodopsin. Light is absorbed by the carotenoid in the transitions from the ground state level S_0 to vibrational sublevels of the second excited state S_2 ($1B_u^+$), 486 nm is the main maximum. The transitions to the first excited state of the carotenoid S_1 ($2^1A_g^-$) are not allowed for symmetry reasons (see most recent review (6)), but this state is populated in internal S_2-to-S_1 conversion. The carotenoid fluorescence with maxima at 529, 564, and 595–600 nm and the energy transfer to the S_1 state of retinal originate from the S_2 state. In analogy with bacteriorhodopsin, the retinal absorption band of xanthorhodopsin (~560 nm at pH 8, and 563 nm at pH 5.5) will be from transition to the Franck-Condon levels of the S_1 state, which is also an acceptor of the energy transferred from salinixanthin. Relaxation of the excited retinal and its environment occurs on a timescale of 100–250 fs (40,69) and leads to a lower-energy excited state (state I) with a lifetime of ~0.5 ps (58), from which the photoreaction and most of the fluorescence emission take place (39,69). Dashed arrows stand for internal conversion of excitation to heat. This is a minimal model. From analogy with other carotenoids (6,82,83) and bacteriorhodopsin (70), one might expect that both chromophores exhibit more excited singlet state levels than shown in this scheme. At least one "dark," symmetry forbidden state ($1B_u^-$) could be present between the S_1 (2^1Ag^-) and S_2 ($1^1B_u^+$) of the carotenoid. The "dark" S_2 (Ag^-) state of the retinal chromophore (55) might be involved in the isomerization process starting from the I state (71–73).

C13=C14 bond in response to the charge redistribution on excitation and change of the bond order (60), which might be responsible for the large Stokes shift of the bacteriorhodopsin and xanthorhodopsin retinal chromophore fluorescence and deviation from the mirror image symmetry of fluorescence and absorption spectrum at low temperature (36,39,61). Branching reactions were proposed to operate even at this early stage, directing part of the molecules back to the initial state (through a nonreactive coordinate) and the other fraction to the photoproduct K through the I state (62). Fluorescence competes with and is quenched by the photoreaction, indicating that both processes occur from the same state (39,61), so the I state is the precursor of the isomerization (59). The lifetime of the I state is in the order of 500 fs (58,63,64). Two other components, with shorter and longer decay times, were observed also (65,66). From the quantum efficiency of the fluorescence, which for bacteriorhodopsin is in the range of 10^{-4} to 2.5×10^{-4} (36,39,42) and radiative lifetime of 7 ns (estimated from the absorption spectrum), the expected lifetime of the excited state is between 0.7 and 1.7 ps, in reasonably good agreement with the experiment. For xanthorhodopsin a 2.5-fold higher quantum yield of fluorescence at pH 8 implies a longer lifetime of the excited state. The photoisomerization in bacteriorhodopsin was described as a transition between just two states, S_1 and S_0 (64,67–69), or as a transition involving all three low-lying electronic states (S_2, S_1, and S_0) (70–74).

Implications for the structure of xanthorhodopsin

The fast and efficient energy transfer in xanthorhodopsin suggests close proximity of the two chromophores. Some rough estimates of the geometry of the two chromophores can be made based on data obtained in this study. It is reasonable to assume that the transition moments are roughly aligned (but not necessarily fully colinear) with the rigid conjugated polyene chains of the chromophores. Thus, in the case of rhodopin glucoside in the light-harvesting complex LH2 of purple bacteria, the deviation of the dipole moment is 9.1° off from the polyene axis (75,76). In bacteriorhodopsin the all-*trans*-retinal is tilted 21.3° from the membrane plane (77), similar to the orientation of the transition dipole moment (78). The high degree of homology of residues in the binding sites of the two proteins (10) suggests that the retinal will be oriented similarly in xanthorhodopsin. In this case, the carotenoid will be tilted either 13° or 55° to the membrane normal. The former orientation is nearly parallel with the transmembrane helices. The angle between the carotenoid and retinal seems a compromise between the best efficiency for energy transfer (parallel) and the ability to collect incident light by the dual-chromophore system at all angles of polarization (perpendicular).

The crystal structure of bacteriorhodopsin (77) would allow placing a large molecule with a long conjugated chain such as salinixanthin along the tightly packed seven-helical bundle. Alignment of the carotenoid with the helical axes, as suggested by the fluorescence polarization, would be consistent with this idea. An interesting question is whether such a location would allow a ~50% efficiency for the energy transfer. The distance between the centers of the two chromophores can be roughly estimated from the spectral features of the salinixanthin antenna and the retinal, assuming that the electronic coupling between the two chromophores can be approximated by interaction of the transition dipole moments of the donor and acceptor; that is, the Förster mechanism (79) can be applied. From Förster treatment, the distance R_o, for 50% energy transfer, is calculated as

$$R_o = 0.21(\kappa^2 n^{-4} \varphi_f \, \text{J})^{1/6}, \qquad (7)$$

where $J = \int F_c(\lambda)\varepsilon_r(\lambda)\lambda^4 d\lambda / (\int F_c(\lambda)d\lambda)$ is the overlap integral of the antenna carotenoid fluorescence spectrum, F_c, and the retinal chromophore absorption spectrum, ε_r. The factor κ^2 depends on the mutual orientation of the donor and acceptor. In the case of xanthorhodopsin, κ^2 is ~0.6. For a maximum extinction of the retinal similar to that of the chromophore of bacteriorhodopsin (60,000 M^{-1} cm^{-1}), a refractive index $n = 1.45$, and a quantum yield for the antenna carotenoid fluorescence ϕ_f of 4×10^{-5}, R_o is ~11 Å.

This calculated distance is shorter than the dimensions of the conjugated chains of the chromophores, particularly for salinixanthin, which is >20 Å long. Energy transfer between such extended but closely located chromophores cannot be described precisely by the simple relation used but requires more detailed knowledge of the spatial arrangement of the two chromophores and the changes of the transition densities, as was shown for carotenoid-to-chlorophyll energy transfer in photosynthetic light-harvesting complexes (80). This information is currently missing for xanthorhodopsin. Nevertheless, the rough estimate of 11 Å locates the carotenoid within the protein or at a protein-lipid interface, at a location consistent with a specific binding site for salinixanthin that interacts with and is controlled by the retinal chromophore (21,27). These estimates are interesting to compare with the recently obtained high-resolution crystal structure of archaerhodopsin (81). This archaeal retinal protein also contains one carotenoid molecule per retinal, in this case bacterioruberin, but with no antenna function (22). The carotenoid is oriented roughly along the helices, on the lipid/protein interface, but inclined at a 50° angle from the retinal. The closest distance to the retinal is 17 Å, which is too far for efficient energy transfer. The function of bacterioruberin is apparently one of photoprotection and structural stabilization.

In conclusion, the fluorescence studies provide direct evidence for the antenna function of salinixanthin in xanthorhodopsin and supply information about the spatial arrangement of the carotenoid relative to the retinal, their excited states, and the pathway of energy transfer. As the simplest light-harvesting system, this unique protein with a

dual chromophore fills the gap between light transducers with a single chromophore, such as bacteriorhodopsin, and the highly complex multipigment multiprotein photosynthetic assemblies. The earliest appearance of carotenoids may have been in the cell membrane of the archaea, where they have photoprotective and possibly structural functions. The carotenoid bacterioruberin binds to archaerhodopsin (21,23) but not near the retinal and does not serve as a light-harvesting antenna (22,23). Closer interaction with the retinal, a more specific binding site, and efficient energy transfer from carotenoid to retinal apparently developed only later in evolution. In the eubacterial retinal-based proton pump xanthorhodopsin, it allows light harvesting in a broader spectral range than possible with a single retinal chromophore and absorbs light at all polarizations. Excitation energy transfer occurs from the short-lived S_2 excited state of salinixanthin to the S_1 state of retinal. A high efficiency is ensured by the short distance between the centers of the conjugated chains of ~ 11 Å and the $\sim 56°$ between their transition dipole moments.

REFERENCES

1. Green, B. R., and W. W. Parson, editors. 2003. Light-Harvesting Antennas in Photosynthesis. Kluwer Academic Publishers, Dordrecht.

2. McDermott, G., S. M. Prince, A. A. Freer, A. M. Hawthornthwaite-Lawless, M. Z. Papiz, R. J. Cogdell, and N. W. Isaacs. 1995. Crystal structure of an integral membrane light-harvesting complex from photosynthetic bacteria. *Nature.* 374:517–521.

3. Frank, H. A. 1999. Incorporation of carotenoids into reaction center and light-harvesting pigment-protein complexes. *In* The Photochemistry of Carotenoids. H. A. Frank, A. J. Young, G. Britton, and R. J. Cogdell, editors. Kluwer Academic Publishers, Dordrecht. 223–234.

4. Kandori, H., H. Sasabe, and M. Mimuro. 1994. Direct determination of a lifetime of the S_2 state of β-carotene by femtosecond time-resolved fluorescence spectroscopy. *J. Am. Chem. Soc.* 116:2671–2672.

5. De Weerd, F. L., J. T. M. Kennis, J. P. Dekker, and R. van Grondelle. 2003. β-Carotene to chlorophyll singlet energy transfer in the photosystem I core of *Synechococcus elongatus* proceeds via the β-carotene S_2 and S_1 states. *J. Phys. Chem. B.* 107:5995–6002.

6. Polivka, T., and V. Sundström. 2004. Ultrafast dynamics of carotenoid excited states—from solution to natural and artificial systems. *Chem. Rev.* 104:2021–2071.

7. Melkozernov, A. N., J. Barber, and R. E. Blankenship. 2006. Light harvesting in photosystem I supercomplexes. *Biochemistry.* 45:331–345.

8. Schulten, K., and M. Karplus. 1972. On the origin of a low-lying forbidden transition in polyenes and related molecules. *Chem. Phys. Lett.* 14:305–309.

9. Hudson, B. S., and B. E. Kohler. 1972. A low-lying weak transition in the polyene $\alpha\omega$-diphenyloctatetraene. *Chem. Phys. Lett.* 14:299–304.

10. Balashov, S. P., E. S. Imasheva, V. A. Boichenko, J. Antón, J. M. Wang, and J. K. Lanyi. 2005. Xanthorhodopsin: a proton pump with a light-harvesting carotenoid antenna. *Science.* 309:2061–2064.

11. Oesterhelt, D., and W. Stoeckenius. 1973. Functions of a new photoreceptor membrane. *Proc. Natl. Acad. Sci. USA.* 70:2853–2857.

12. Litvin, F. F., V. A. Boichenko, S. P. Balashov, and V. T. Dubrovskii. 1977. Photoinduced inhibition and stimulation of respiration in cells of *Halobacterium halobium*: kinetics, action spectra, relation to photoinduction of ΔpH. *Biofizika.* 22:1062–1071.

13. Kirschfeld, K., N. Franceschini, and B. Minke. 1977. Evidence for a sensitising pigment in fly photoreceptors. *Nature.* 269:386–390.

14. Stark, W. S., and K. E. W. P. Tan. 1982. Ultraviolet light: photosensitivity and other effects of the visual system. *Photochem. Photobiol.* 36:371–380.

15. Douglas, R. H., J. C. Partridge, K. Dulai, D. Hunt, C. W. Mullineaux, A. Y. Tauber, and P. H. Hynninen. 1998. Dragon fish see using chlorophyll. *Nature.* 393:423–424.

16. Isayama, T., D. Alexeev, C. L. Makino, I. Washington, K. Nakanishi, and N. J. Turro. 2006. An accessory chromophore in red vision. *Nature.* 443:649.

17. Sineshchekov, O. A., and F. F. Litvin. 1988. Mechanisms of phototaxis of microorganisms. *In* Molecular Mechanisms of Biological Effects of Optical Radiation (in Russian). A. B. Rubin, editor. Nauka, Moscow. 212–227.

18. Litvin, F. F., O. A. Sineshchekov, and V. A. Sineshchekov. 1978. Photoreceptor electric potential in the phototaxis of the alga *Haematococcus pluvialis*. *Nature.* 271:476–478.

19. Lutnaes, B. F., A. Oren, and S. Liaaen-Jensen. 2002. New C_{40}-carotenoid acyl glycoside as principal carotenoid in *Salinibacter ruber*, an extremely halophilic eubacterium. *J. Nat. Prod.* 65:1340–1343.

20. Balashov, S. P., and J. K. Lanyi. 2007. Xanthorhodopsin: proton pump with a carotenoid antenna. *Cell. Mol. Life Sci.* 64:2323–2328.

21. Balashov, S. P., E. S. Imasheva, and J. K. Lanyi. 2006. Induced chirality of light-harvesting carotenoid salinixanthin and its interaction with the retinal of xanthorhodopsin. *Biochemistry.* 45:10998–11004.

22. Boichenko, V. A., J. M. Wang, J. Antón, J. K. Lanyi, and S. P. Balashov. 2006. Functions of carotenoids in xanthorhodopsin and archaerhodopsin, from action spectra of photoinhibition of cell respiration. *Biochim. Biophys. Acta.* 1757:1649–1656.

23. Mukohata, Y., K. Ihara, K. Uegaki, Y. Miyashita, and Y. Sugiyama. 1991. Australian *Halobacteria* and their retinal-protein ion pumps. *Photochem. Photobiol.* 54:1039–1045.

24. Béjà, O., E. N. Spudich, J. L. Spudich, M. Leclerc, and E. F. DeLong. 2001. Proteorhodopsin phototrophy in the ocean. *Nature.* 411:786–789.

25. Mongodin, E. F., K. E. Nelson, S. Daugherty, R. T. DeBoy, J. Wister, H. Khouri, J. Weidman, D. A. Walsh, R. T. Papke, G. Sanchez Perez, A. K. Sharma, C. L. Nesbø, D. MacLeod, E. Bapteste, W. F. Doolittle, R. L. Charlebois, B. Legault, and F. Rodriguez-Valera. 2005. The genome of *Salinibacter ruber*: convergence and gene exchange among hyperhalophilic bacteria and archaea. *Proc. Natl. Acad. Sci. USA.* 102:18147–18152.

26. Antón, J., A. Oren, S. Benlloch, F. Rodríguez-Valera, R. Amann, and R. Rosselló-Mora. 2002. *Salinibacter ruber* gen. nov., sp. nov., a novel, extremely halophilic member of the *Bacteria* from saltern crystallizer ponds. *Int. J. Syst. Evol. Microbiol.* 52:485–491.

27. Imasheva, E. S., S. P. Balashov, J. M. Wang, E. Smolensky, M. Sheves, and J. K. Lanyi. 2008. Chromophore interaction in xanthorhodopsin—retinal dependence of salinixanthin binding. *Photochem. Photobiol.* 84:977–984.

28. Peters, J., R. Peters, and W. Stoeckenius. 1976. A photosensitive product of sodium borohydride reduction of bacteriorhodopsin. *FEBS Lett.* 61:128–134.

29. Schreckenbach, T., B. Walckhoff, and D. Oesterhelt. 1977. Studies on the retinal-protein interaction in bacteriorhodopsin. *Eur. J. Biochem.* 76:499–511.

30. Schreckenbach, T., B. Walckhoff, and D. Oesterhelt. 1978. Specificity of the retinal binding site of bacteriorhodopsin: chemical and stereochemical requirements for the binding of retinol and retinal. *Biochemistry.* 17:5353–5359.

31. Lakowicz, J. R. 2006. Principles of Fluorescence Spectroscopy. Springer, Singapore.

32. Koyama, Y. 1995. Resonance Raman spectroscopy. *In* Carotenoids. G. Britton, S. Liaaen-Jensen, and H. Pfander, editors. Birkhäuser Verlag, Basel,. 135–146.

33. Strickler, S. J., and R. A. Berg. 1962. Relationship between absorption intensity and fluorescence lifetime of molecules. *J. Chem. Phys.* 37: 814–822.

34. Heyn, M. P., R. J. Cherry, and U. Müller. 1977. Transient and linear dichroism studies on bacteriorhodopsin: determination of the orientation of the 568 nm all-*trans* retinal chromophore. *J. Mol. Biol.* 117: 607–620.

35. Ebrey, T. G., B. Becher, B. Mao, P. Kilbride, and B. Honig. 1977. Exciton interactions and chromophore orientation in purple membrane. *J. Mol. Biol.* 112:377–397.

36. Lewis, A., J. P. Spoonhower, and G. J. Perreault. 1976. Observation of light emission from a rhodopsin. *Nature.* 260:675–678.

37. Sineshchekov, V. A., and F. F. Litvin. 1977. Luminescence of bacteriorhodopsin from *Halobacterium halobium* and its connection with photochemical conversions of the chromophore. *Biochim. Biophys. Acta.* 462:450–466.

38. Govindjee, R., and T. G. Ebrey. 1986. Light emission from bacteriorhodopsin and rhodopsin. *In* Light Emission by Plants and Bacteria. R. Govindjee, J. Amesz, and D. Fork, editors. Academic Press, Orlando. 401–419.

39. Balashov, S. P., F. F. Litvin, and V. A. Sineshchekov. 1988. Photochemical processes of light energy transformation in bacteriorhodopsin. *In* Physicochemical Biology Reviews. V. P. Skulachev, editor. Harwood Academic Publishers, Reading, UK. 1–61.

40. Kennis, J. T. M., D. S. Larsen, K. Ohta, M. T. Facciotti, R. M. Glaeser, and G. R. Fleming. 2002. Ultrafast protein dynamics of bacteriorhodopsin probed by photon echo and transient absorption spectroscopy. *J. Phys. Chem. B.* 106:6067–6080.

41. Imasheva, E. S., S. P. Balashov, J. M. Wang, and J. K. Lanyi. 2006. pH-dependent transitions in xanthorhodopsin. *Photochem. Photobiol.* 82:1406–1413.

42. Kouyama, T., K. Kinosita, and A. Ikegami. 1985. Excited-state dynamics of bacteriorhodosin. *Biophys. J.* 47:43–54.

43. Song, L., M. A. El-Sayed, and J. K. Lanyi. 1993. Protein catalysis of the retinal subpicosecond photoisomerization in the primary process of bacterial photosynthesis. *Science.* 261:891–894.

44. Frank, H. A., and R. J. Cogdell. 1993. The photochemistry and function of carotenoids in photosynthesis. *In* Carotenoids in Photosynthesis. A. Young, and G. Britton, editors. Chapman and Hall, London. 252–326.

45. DeCoster, B., R. L. Christensen, R. Gebhard, J. Lugtenburg, R. Farhoosh, and H. A. Frank. 1992. Low-lying electronic states of carotenoids. *Biochim. Biophys. Acta.* 1102:107–114.

46. Christensen, R. L. 1999. The electronic states of carotenoids. *In* The Photochemistry of Carotenoids. H. A. Frank, A. J. Young, G. Britton, and R. J. Cogdell, editors. Kluwer Academic Publishers, Dordrecht. 137–157.

47. Fujii, R., K. Onaka, H. Nagae, Y. Koyama, and Y. Watanabe. 2001. Fluorescence spectroscopy of all-*trans*-lycopene: comparison of the energy and the potential displacements of its $2A_g^-$ state with those of neurosporene and spheroidene. *J. Lumin.* 92:213–222.

48. Henderson, R., and P. N. Unwin. 1975. Three-dimensional model of purple membrane obtained by electron microscopy. *Nature.* 257:28–32.

49. El-Sayed, M. A., C. T. Lin, and W. R. Mason. 1989. Is there an excitonic interaction or antenna system in bacteriorhodopsin? *Proc. Natl. Acad. Sci. USA.* 86:5376–5379.

50. Rondonuwu, F. S., K. Yokoyama, R. Fujii, Y. Koyama, R. J. Cogdell, and Y. Watanabe. 2004. The role of the $1^1B_u^-$ state in carotenoid-to-bacteriochlorophyll singlet-energy transfer in the LH2 antenna complexes from *Rhodobacter sphaeroides* G1C, *Rhodobacter sphaeroides* 2.4.1, *Rhodospirillum molischianum* and *Rhodopseudomonas acidophila*. *Chem. Phys. Lett.* 390:314–322.

51. Akahane, J., F. S. Rondonuwu, L. Fiedor, Y. Watanabe, and Y. Koyama. 2004. Dependence of singlet-energy transfer on the conjugation length of carotenoids reconstituted into the LH1 complex from *Rhodospirillum rubrum* G9. *Chem. Phys. Lett.* 393:184–191.

52. Furuichi, K., T. Sashima, and Y. Koyama. 2002. The first detection of the $3A_g^-$ state in carotenoids using resonance-Raman excitation profiles. *Chem. Phys. Lett.* 356:547–555.

53. Holt, N. E., J. T. M. Kennis, and G. R. Fleming. 2004. Femtosecond fluorescence upconversion studies of light harvesting by β-carotene in oxygenic photosynthetic core proteins. *J. Phys. Chem. B.* 108:19029–19035.

54. Schulten, K., U. Dinur, and B. Honig. 1980. The spectra of carbonium ions, cyanine dyes, and protonated Schiff base polyenes. *J. Chem. Phys.* 73:3927–3935.

55. Birge, R. R. 1990. Nature of the primary photochemical events in rhodopsin and bacteriorhodopsin. *Biochim. Biophys. Acta.* 1016:293–327.

56. Yamaguchi, S., and H. Hamaguchi. 1998. Femtosecond ultraviolet-visible absorption study of all-*trans* → 13-*cis* · 9-*cis* photoisomerization of retinal. *J. Chem. Phys.* 109:1397–1408.

57. Birge, R. R., and C.-F. Zhang. 1990. Two-proton double resonance spectroscopy of bacteriorhodopsin. Assignment of the electronic and dipolar properties of the low-lying $^1A_g^*$-like and $^1B_u^{*+}$-like π, π* states. *J. Chem. Phys.* 92:7178–7195.

58. Sharkov, A. V., A. V. Pakulev, S. V. Chekalin, and Y. A. Matveetz. 1985. Primary events in bacteriorhodopsin probed by subpicosecond spectroscopy. *Biochim. Biophys. Acta.* 808:94–102.

59. Ruhman, S., B. Hou, N. Friedman, M. Ottolenghi, and M. Sheves. 2002. Following evolution of bacteriorhodopsin in its reactive excited state via stimulated emission pumping. *J. Am. Chem. Soc.* 124:8854–8858.

60. Song, L., and M. A. El-Sayed. 1998. Primary step in bacteriorhodopsin photosynthesis: Bond stretch rather than angle twist of its retinal excited-state structure. *J. Am. Chem. Soc.* 120:8889–8890.

61. Sineshchekov, V. A., S. P. Balashov, and F. F. Litvin. 1981. Fluorescence of photoactive bacteriorhodopsin. *Biofizika.* 26:964–972.

62. Aharoni, A., B. Hou, N. Friedman, M. Ottolenghi, I. Rousso, S. Ruhman, M. Sheves, T. Ye, and Q. Zhong. 2001. Non-isomerizable artificial pigments: implications for the primary light-induced events in bacteriorhodopsin. *Biochemistry (Mosc.).* 66:1210–1219.

63. Sharkov, A. V., Y. A. Matveetz, S. V. Chekalin, A. V. Konyashchenko, O. M. Brekhov, and B. Y. Rootskoy. 1983. Fluorescence of bacteriorhodopsin under subpicosecond light excitation. *Photochem. Photobiol.* 38:108–111.

64. Mathies, R. A., C. H. Brito-Cruz, W. T. Pollard, and C. V. Shank. 1988. Direct observation of the femtosecond excited-state *cis-trans* isomerization in bacteriorhodopsin. *Science.* 240:777–779.

65. Du, M., and G. R. Fleming. 1993. Femtosecond time-resolved fluorescence spectroscopy of bacteriorhodopsin—direct observation of excited-state dynamics in the primary step of the proton pump cycle. *Biophys. Chem.* 48:101–111.

66. Schmidt, B., C. Sobotta, B. Heinz, S. Laimgruber, M. Braun, and P. Gilch. 2005. Excited-state dynamics of bacteriorhodopsin probed by broadband femtosecond fluorescence spectroscopy. *Biochim. Biophys. Acta.* 1706:165–173.

67. Hayashi, S., E. Tajkhorshid, and K. Schulten. 2003. Molecular dynamics simulation of bacteriorhodopsin's photoisomerization using ab initio forces for the excited chromophore. *Biophys. J.* 85:1440–1449.

68. Kochendoerfer, G. G., and R. A. Mathies. 1995. Ultrafast spectroscopy of rhodopsins—photochemistry at its best. *Isr. J. Chem.* 35:211–226.

69. McCamant, D. W., P. Kukura, and R. A. Mathies. 2005. Femtosecond stimulated Raman study of excited-state evolution in bacteriorhodopsin. *J. Phys. Chem. B.* 109:10449–10457.

70. Hasson, K. C., F. Gai, and P. A. Anfinrud. 1996. The photoisomerization of retinal in bacteriorhodopsin: experimental evidence for a three-state model. *Proc. Natl. Acad. Sci. USA.* 93:15124–15129.

71. Gai, F., K. C. Hasson, J. C. McDonald, and P. A. Anfinrud. 1998. Chemical dynamics in proteins: the photoisomerization of retinal in bacteriorhodopsin. *Science.* 279:1886–1891.

72. Humphrey, W., H. Lu, I. Logunov, H. J. Werner, and K. Schulten. 1998. Three electronic state model of the primary phototransformation of bacteriorhodopsin. *Biophys. J.* 75:1689–1699.

73. Kobayashi, T., T. Saito, and H. Ohtani. 2001. Real-time spectroscopy of transition states of bacteriorhodopsin during retinal isomerization. *Nature.* 414:531–534.

74. Kobayashi, T., A. Yabushita, T. Saito, H. Ohtani, and M. Tsuda. 2007. Sub-5-fs real-time spectroscopy of transition states in bacteriorhodopsin during retinal isomerization. *Photochem. Photobiol.* 83:363–368.

75. Georgakopoulou, S., R. J. Cogdell, R. van Grondelle, and H. van Amerongen. 2003. Linear-dichroism measurements on the LH2 antenna complex of *Rhodopseudomonas acidophila* strain 10050 show that the transition dipole moment of the carotenoid rhodopin glucoside is not collinear with the long molecular axis. *J. Phys. Chem. B.* 107:655–658.

76. Dolan, P. M., D. Miller, R. J. Cogdell, R. R. Birge, and H. A. Frank. 2001. Linear dichroism and the transition dipole moment orientation of the carotenoid in the LH2 antenna complex in membranes of *Rhodopseudomonas acidophila* strain 10050. *J. Phys. Chem. B.* 105: 12134–12142.

77. Luecke, H., B. Schobert, H.-T. Richter, J.-P. Cartailler, and J. K. Lanyi. 1999. Structure of bacteriorhodopsin at 1.55 Å resolution. *J. Mol. Biol.* 291:899–911.

78. Heyn, M. P., B. Borucki, and H. Otto. 2000. Chromophore reorientation during the photocycle of bacteriorhodopsin: experimental methods and functional significance. *Biochim. Biophys. Acta.* 1460:60–74.

79. Förster, T. 1946. Energiewanderung und fluoreszenz. *Naturwissenschaften.* 6:166–175.

80. Krueger, B. P., G. D. Scholes, and G. R. Fleming. 1998. Calculation of couplings and energy-transfer pathways between the pigments of LH2 by the ab initio transition density cube method. *J. Phys. Chem. B.* 102:5378–5386.

81. Yoshimura, K., and T. Kouyama. 2008. Structural role of bacterioruberin in the trimeric structure of archaerhodopsin-2. *J. Mol. Biol.* 375:1267–1281.

82. Tavan, P., and K. Schulten. 1987. Electronic excitations in finite and infinite polyenes. *Phys. Rev. B.* 36:4337–4358.

83. Koyama, Y., F. S. Rondonuwu, and R. Fujii. 2004. Light-harvesting function of carotenoids in photosynthesis: the roles of newly found $1^1B_u^-$ state. *Biopolymers.* 74:2–18.